PROCEEDINGS OF SCIENCE

Cosmic Rays origin studies in the W44 region with *Fermi*-LAT and MAGIC observations

Di Tria R.,[a,b,*] **Di Venere L.,**[b] **Giordano F.,**[a,b] **Green D.,**[c] **Hahn A.,**[c] **Morlino G.,**[d] **Pantaleo F.R.**[a,b] **and Strzys M.**[e] **on behalf of the *Fermi*-LAT and MAGIC Collaborations**

[a] *Dipartimento Interateneo di Fisica dell'Università e del Politecnico di Bari, via Orabona 4, 70125, Bari, Italy*

[b] *INFN Sezione di Bari, via Orabona 4, 70125, Bari, Italy*

[c] *Max-Planck-Institut for Physics, Föhringer Ring 6, 80805, München, Germany*

[d] *INAF Osservatorio Astronomico di Arcetri, Largo Enrico Fermi 5, 50125, Firenze, Italy*

[e] *Institute for Cosmic Ray Research 1035 (ICRR), The University of Tokyo, Kashiwa, 277-8582 Chiba, Japan*

E-mail: riccardo.ditria@uniba.it

W44 is a well-known Supernova Remnant (SNR) observed in high-energy gamma-rays, widely studied to investigate cosmic ray (CR) acceleration. Several analyses of the W44 surroundings showed the presence of a gamma-ray emission offset from the radio SNR shell. This emission is thought to originate from escaped high-energy CRs.

We present a detailed analysis of the W44 region as seen by Fermi-LAT, focusing on the spatial and spectral characteristics of both W44 SNR and its surroundings. The spatial analysis was limited to energies above 1 GeV in order to exploit the improved angular resolution of the instrument, deriving a detailed description of the region morphology. The spectral analysis was extended down to 100 MeV, favouring the hadronic origin of gamma-rays. Observations of the North-Western region of W44 were conducted with the MAGIC telescopes in the very-high-energy gamma-ray band. We analysed MAGIC data above 130 GeV exploiting the spatial information derived from the Fermi-LAT analysis above 1 GeV.

Here we show the results of both analyses and the combined Fermi-LAT and MAGIC spectra. An interpretation model was developed, assuming that the gamma-ray emission from the surroundings is due to clouds located near W44 and illuminated by CRs escaping along the SNR's magnetic field lines, thus obtaining constraining information on the diffusion coefficient of the escaped CRs.

7th Heidelberg International Symposium on High-Energy Gamma-Ray Astronomy (Gamma2022)
4-8 July 2022
Barcelona, Spain

*Speaker

PoS(Gamma2022)044

1. Introduction

Supernova remnants (SNRs) are considered very strong candidates as birthplaces of Cosmic Rays (CRs), in particular in Galactic environments. W44, an extended middle-aged SNR ($\sim 2 \cdot 10^4$ yr), is one of the strongest gamma-ray emitters in the Milky Way. Indeed, AGILE and *Fermi* Large Area Telescope (LAT) reported its high energy (HE) emission with strong evidence of hadronic interaction of accelerated CRs with the dense environment [1, 2]. Moreover previous works revealed HE emission also in the area surrounding the SNR. Authors in [2] discovered GeV emission from two extended regions, close to the W44 shell, thought to originate from escaped CRs interacting with the dense medium, hypothesis also confirmed by [3].

In this contribution, we present the updated results of the observations of the W44 region with *Fermi*-LAT at energies above 100 MeV, together with observations of the North-Western region of W44 with the MAGIC telescopes at energies above 130 GeV. Finally we developed an interpretation model based on acceleration and escape of particles from the forward shock of the SNR.

2. *Fermi*-LAT analysis

The LAT instrument onboard the Fermi satellite is a pair-conversion telescope with a precision converter-tracker and a calorimeter, sensitive to gamma rays from tens of MeV to a few TeV.

We selected almost 12 years of `Pass8_R3` data from a Region of Interest (RoI) of 15° centered on the W44 position (GLON: 34.65°, GLAT: -0.38°). We performed a binned summed likelihood analysis in a squared region inscribed in the RoI selected. Data were binned in pixels of 0.1° and in energy bins equally spaced in logarithmic scale considering 8 bins/decade. We selected `SOURCE` class events and we divided the dataset according to the `PSF` event types. In order to get rid of the Earth limb contamination we applied a cut on the maximum zenith angle, adapting the choice of z_{max} to the energy range analyzed following the prescriptions of the *Fermi*-LAT collaboration reported in [4].

The RoI was modelled including all the known sources from the 4FGL-DR2 catalog [4] within 20° from the RoI center and the Galactic and isotropic diffuse background models[1]. The normalization parameters of the diffuse components and of sources having a Test Statistics (TS) larger than 20 were fitted, while other parameters were kept fixed at the catalog values. The analysis was conducted using the *fermitools* (v2.0.8) and the *fermipy* (v1.0.1) package.

A detailed morphological analysis of the W44 region was conducted selecting `PSF2` and `PSF3` events with energy above 1 GeV and with a maximum zenith angle of 105°. All known sources within 1° from the RoI center, except for W44, were removed and a source-find algorithm was applied to detect new point-like sources having a significance above 5σ. For the newly found sources an *extension* test was performed, in order to determine whether a disk model was more suitable than a point-like model, and a *curvature* test, in order to determine whether a `Log-Parabola` spectrum[2] was more suitable than a `power-law` spectrum. This procedure was repeated for different spatial templates employed for the W44 SNR. For each analysis result the *Akaike Information Criterion (AIC)* [6] $AIC = 2k - 2lnL$, with k the number of free parameters of the model, was evaluated. The

[1] See https://fermi.gsfc.nasa.gov/ssc/data/access/lat/BackgroundModels.html for more details.
[2] https://fermi.gsfc.nasa.gov/ssc/data/analysis/scitools/source_models.html

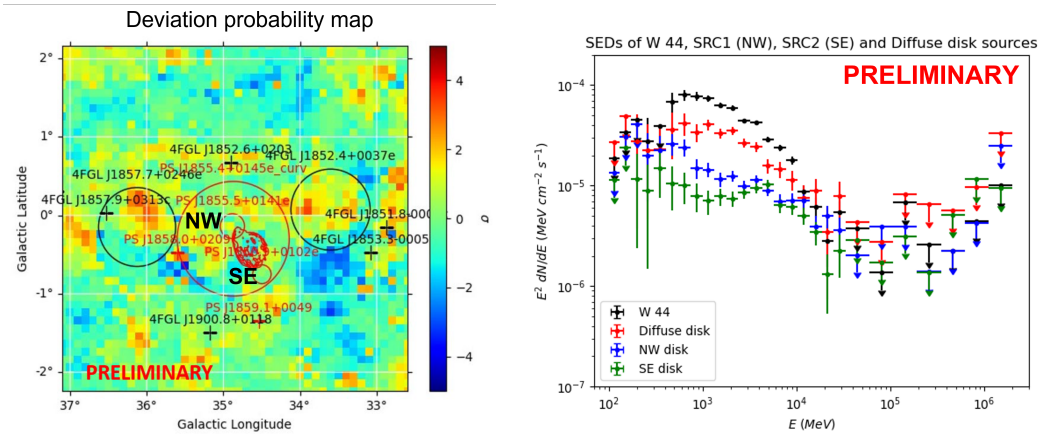

Figure 1: Left: deviation probability map, or *PS map*, in σ units of W44 surroundings derived from the analysis above 1 GeV. Red contours represent the W44 radio template. The red crosses and red circles show the new sources added in this analysis, while the black ones correspond to sources in the 4FGL-DR2 *Fermi*-LAT catalog. The radii of the circles represent the r_{68} of the sources, i.e. the 68% containment radii of their best-fit spatial models. Right: SEDs of the W44 SNR, of the nearby sources NW and SE and of the large diffuse disk derived with *Fermi*-LAT data.

templates considered as spatial models of W44 were: the 4FGL catalog template, derived in [7], a radio (1420 MHz) template derived from the THOR survey [8] and a full-ellipse template, result of a dedicated analysis [9] and characterized by an inclination angle of 115° and semi-axes a = 0.41° and b = 0.23°. The catalog template and the full-ellipse template were also divided along the major axis, with the two half-ellipses fitted as independent sources. The radio template provided the minimum value of the AIC, hence was chosen as spatial model of W44. Two moderately extended sources were detected and associated to the North-West (NW) and South-East (SE) sources observed in previous works [2, 3], with a spatial extension of 0.19° ± 0.01 and 0.15° ± 0.01, respectively. Moreover an extended central source, modelled as a large disk, was added to describe a residual diffuse γ-ray emission. Fig.1(left) shows a deviation probability map[3] converted in σ units, showing no significant deviation in the region close to the W44 SNR.

The low-energy spectral analysis was conducted over the whole energy range, from 100 MeV to 2 TeV, performing a weighted likelihood fit which allows to mitigate the effects of the systematic errors mainly due to an imperfect knowledge of the Galactic background emission and is based on the work reported in [5] and Appendix B of [4]. The analysis was conducted considering the best morphology of the RoI, from the HE analysis, and repeating the curvature fitting procedure on the sources of interest. In Fig.1(right) are reported the Spectral Energy Distributions calculated for W44 and for the three surrounding sources over 8 bins/decade for energies up to 30 GeV and over 4 bins/decade for energies above 30 GeV.

[3]The deviation probability map, or *PS map*, shows the data/model agreement and is sensitive to both positive and negative fluctuations. The *PS* is defined as $|PS| = -\log 10(p - value)$ and values of 2.57, 4.2, 6.24 correspond to a significance of 3, 4, 5 σ, respectively. See here for more details https://indico.cern.ch/event/1010947/contributions/4278096/attachments/2228212/3774978/bruel_FermiSymposium2021_PSmap_v4.pdf

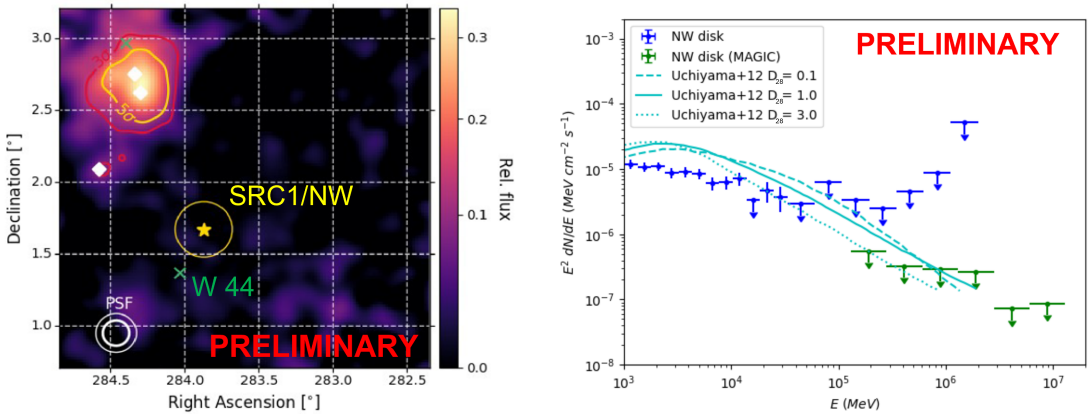

Figure 2: Left: relative flux map of the region observed with the MAGIC telescopes. The modelled sources MAGIC J1857.2+0263 and MAGIC J1857.6+0297 are marked with white diamonds. The green cross marks the center of W44. The yellow circle indicates the extension of the NW source. Right: SED of the NW source evaluated from the *Fermi*-LAT (blue) and MAGIC (green) data. In light blue the γ-ray emission, derived in [2], in case of CRs escaped from W44 and illuminating a nearby cloud for three values of the diffusion coefficient obtained from Eq. 4 of [2] with D_{28} = 0.1, 1.0, 3.0.

3. MAGIC analysis

The MAGIC collaboration operates a stereoscopic system of two IACTs on the Canary island of La Palma [11]. Between 2013 and 2014, MAGIC observed the W44 region for a total of 173.7 h after quality cuts. The observations were performed in so-called wobble mode with 0.4° offset, centered on the coordinates of NW from Uchiyama et al. [2]. We used the standard MAGIC analysis software MARS for the low-level analysis [12, 13] and `SkyPrism` [14] for the spacial and spectral analysis. The systematic uncertainties can be estimated from Aleksić et al. [13] and Vovk et al. [14]. In `SkyPrism`, uncertainties can be directly derived from log-likelihood deviations of the obtained fit. We constructed the background using an exclusion map by excluding the sources relevant to MAGIC in its FoV. We excluded a disk of radius 0.45° around HESS J1857+026 [15], which includes MAGIC J1857.2+0263 and MAGIC J1857.6+0297 from [16], a circular region of 0.34° diameter around HESS J1858+020 [15], and sources NW and SE with their respective extensions from the *Fermi*-LAT analysis above. Due to their curved spectra, W44 and the large background components have a negligible contribution in the MAGIC energy range and did not need to be excluded. Figure 2 (left) shows the relative flux map of the region derived from MAGIC data. NW was not detected significantly, thus we derived 95% CL spectral upper limits shown in figure 2 (right).

4. γ-ray emission model

We used a time-dependent model to show that the gamma-ray emission from the W44 SNR and the surrounding sources can be due to particles accelerated in and escaping from the forward shock of the SNR. The presence of the NW and SE sources, both along the major axis of W44, led us to assume that their emission could be associated to hadrons escaping from the remnant along

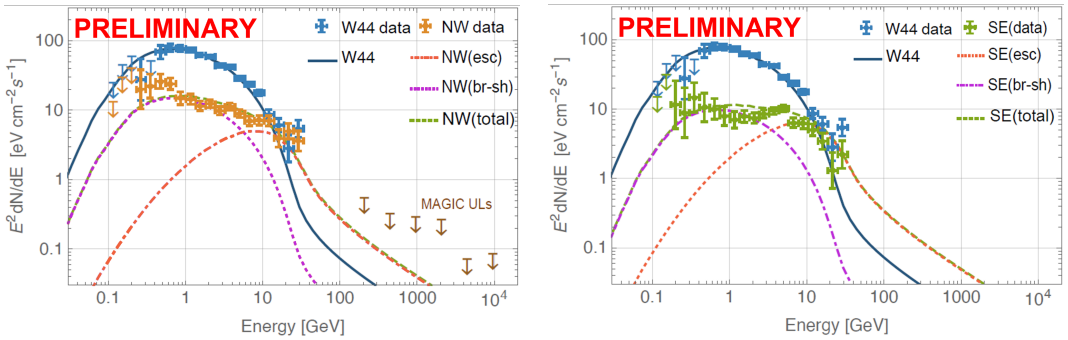

Figure 3: Gamma-ray emissions from NW (left panel) and SE (right) with the low-energy component due to the broken shock (`br-sh`) and high-energy component due to the escape of particles with momentum $p > p_{\rm max}(t_{age}) = 44$ GeV/c. Then green line shows the sum of the two contributions while the blue line is the emission from the SNR interior.

the local magnetic field and illuminating the surrounding clouds. This hypothesis is supported by a recent analysis [17], in which the authors inferred the direction of the large scale magnetic field using the *Velocity Gradient Technique*, which resulted in an orientation along the major axis of the SNR. This could favour an anisotropic escape of the particles along the magnetic field direction.

The acceleration and escape process was modelled following [18] where, however, a full spherical symmetry is assumed. In our case the particles diffusing outside the SNR are located only inside the magnetic flux tube, i.e. assuming a full cylindrical symmetry in the region close to the remnant axis where the clouds are located. The particle densities in the spherical scenario [18] are then scaled by a factor r^2 to account for the different geometry. The assumed distribution function of CRs accelerated at the shock is $f_{\rm sh}(p,t) \propto \xi_{\rm cr} p^{-\alpha} e^{-p/p_{\rm max}(t)}$ where $\xi_{\rm cr}$ is the shock acceleration efficiency assumed constant in time. The particles maximum momentum is assumed to decrease in time following the phenomenological relation $p_{\rm max}(t) = p_M (t/t_{\rm Sed})^{-\delta}$ with p_M and δ free parameters, derived from the gamma-ray flux fitting. The external diffusion coefficient is assumed to be suppressed with respect to the average Galactic one $D_{\rm ext}(p) = \chi D_{\rm gal}(p)$. Assuming for the SNR an age of $t_{age} = 20$ kyr, a distance of 2.2 kpc, a mass of the ejecta of 5 $M_\odot$, an explosion energy of 10^{51} erg and an average circumstellar medium density ~ 10 cm^{-3}, the estimated time $t_{\rm Sed}$ amounts to 420 yr. The values of the free parameters derived from the fit of the gamma-ray spectrum are $\xi_{\rm cr} = 1.3\%$, $\alpha = 4.2$, $p_M = 100$ TeV, $\delta = 2$. From these parameters, the resulting $p_{\rm max}$ at the SNR age is $p_{\rm max}(t_{age}) = 44$ GeV/c. Regarding the surrounding NW and SE sources, assumed to be at the same distance from us as W44, the model reproduces well the emissions above a few GeV and in particular the bump around 10 GeV, for an external diffusion coefficient $D_{\rm ext}(p) = 0.2\, D_{\rm gal}(p)$ and for distances W44 - NW of 17.3 pc and W44 - SE of 15.7 pc. The NW and SE sources are assumed to be spherical (with radii of 7.3 pc and 5.7 pc respectively) and the reported distances are between the SNR shock and the cloud centers.

However, the particle escape scenario (orange lines in Fig.3) underestimates the low energy emission. Therefore, a *broken-shock* scenario is assumed, in which a small fraction of particles at the SNR shock (about 4% for NW source and 1.5% for SE source) can escape from regions where the shock disappears (e.g. for the presence of dense and small clumps) and diffuse outside the SNR with the diffusion coefficient $D_{\rm ext}$. Finally we estimated the time necessary for these particles to fill

the two clouds ($t_{fill} \approx (2R_{NW/SE})^2/2D_{ext}(p)$), which is found to be less than 20% of the remnant age for both clouds. This suggests that the broken shock starts to appear in the last part of the SNR life. The resulting gamma-ray spectrum (purple lines in Fig.3) has the same shape as the SNR, being the spectrum of the accelerated particles the same as the SNR interior. The total emission describes well the observed gamma-ray spectrum of both sources.

5. Summary

We report here on the study of the W44 region performed with *Fermi*-LAT and MAGIC observations. For this work a detailed analysis of the W44 region was performed on almost 12 years of *Fermi*-LAT data above 100 MeV, deriving spatial and spectral information. The spatial parameters were used for the analysis of the data collected with the MAGIC telescopes which observed the North-West region around the SNR. Since no detection was found, upper limits on the differential flux were derived from MAGIC data.

An interpretation model, based on the acceleration and escape of particles from the forward shock of the W44 SNR, explains well the emission above a few GeV. The low-energy component requires a broken-shock scenario, where also a certain amount of lower energy particles are allowed to escape.

We point out that the reported results are preliminary and that a refined version of the analysis and of the interpretation model will be described, in more details, in a paper in preparation.

Acknowledgments

The *Fermi*-LAT Collaboration acknowledges support for LAT development, operation and data analysis from NASA and DOE (United States), CEA/Irfu and IN2P3/CNRS (France), ASI and INFN (Italy), MEXT, KEK, and JAXA (Japan), and the K.A. Wallenberg Foundation, the Swedish Research Council and the National Space Board (Sweden). Science analysis support in the operations phase from INAF (Italy) and CNES (France) is also gratefully acknowledged. This work performed in part under DOE Contract DE-AC02-76SF00515. We also acknowledge the support from the agencies and organizations listed here: https://magic.mpp.mpg.de/ack_public_2022_05/.

References

[1] Giuliani, et al. 2011, ApJL, 742, L30, AAS
[2] Uchiyama, et al. 2012, ApJL, 749, L35, arXiv: 1203.3234
[3] Peron, G., Aharonian, F., Casanova, S., Zanin, R., & Romoli, C. 2020, ApJL, 896, L23, AAS
[4] Abdollahi, S., Acero, F., Ackermann, M., et al. 2020, ApJ Supplement Series, 247, 33, AAS
[5] Ballet, J. 2016, in Proceedings, 34th International Cosmic Ray Conference (ICRC2015), 848
[6] Akaike H., 1998 "A New Look at the Statistical Model Identification", pages 215–222, Springer New York.
[7] Abdo, A. A., et al. Science, 327, February 2010
[8] Beuther, H., Bihr, S., Rugel, M, et al. 2016, A&A, 595, A32
[9] Di Tria, R., et al. 2021, in Proceedings, 37th International Cosmic Ray Conference (ICRC2021), 642
[10] Umemoto, T., et al. 2017, PASJ, 69 (5), doi:10.1093/pasj/psx061.
[11] Aleksić, et al. 2016a, Astroparticle Physics, 72, 61

[12] Zanin, R. 2013, in Proceedings, 33rd International Cosmic Ray Conference (ICRC2013), 0773
[13] Aleksić, et al. 2016b, Astroparticle Physics, 72, 76
[14] Vovk, I., Strzys, M., & Fruck, C. 2018, A&A, 619, A7, EDP Sciences
[15] Abdalla, et al. 2018, A&, 612, A1, EDP Sciences
[16] Aleksić, et al. 2014, A&A, 571, A96
[17] Liu, M., Hu, Y., Lazarian, A., et al. 2022, MNRAS, 510, 4
[18] Celli, S., Morlino, G., Gabici, S., Aharonian, F. A., 2019, MNRAS, 490, 3